High Performance 60 GHz Beamforming Antenna Array For 5G and Beyond Industrial Applications

Abdul Jabbar[1], Qammer Abbasi[1], Zhibo Pang[2], Muhammad Ali Imran[1], Masood Ur Rehman[1]
[1]James Watt School of Engineering, University of Glasgow, United Kingdom
[2]Automation Technology, ABB, Vasteras, Sweden
a.jabbar.1@research.gla.ac.uk

***Abstract*—A compact and high-performance beamforming array antenna is designed for 60 GHz Industrial, Scientific, and Medical (ISM) band industrial applications. The proposed 16-element array provides peak realized gain of 16.5 dBi and half power beamwidth of 7° at 61 GHz (with realized gain greater than 15 dBi in the achieved band of 57-64 GHz). Radiation efficiency is greater than 70% in the band. The side-lobe levels are less than -10 dB in E and H planes, with extremely low cross-polarization levels. Since the design of a low loss and wideband feed network is a challenging task at mmWave bands, therefore the junction lengths and chamfered transitions of the power divider are carefully optimized to achieve enhanced array performance, and a thorough analysis is presented. Moreover, an accurate antenna connector model is co-simulated and analyzed, which significantly affects antenna performance at millimeter wave bands. Measured and simulated results show good agreement.**

***Index Terms*—60 GHz antenna, beamforming array, industrial communication, millimeter-wave antenna.**

I. Introduction

Millimeter-wave (mmWave) communication is considered as one of the enabling technologies to envision fifth-generation (5G) and sixth-generation (6G) based industrial communication networks [1]–[3]. With the proliferation of 5G and beyond communication systems, the industrial paradigm has shifted towards Industry 4.0 and beyond [4]. Sophisticated 5G and 6G-based industrial applications, such as high-definition video signals, intelligent logistics, intelligent manufacturing, remote visual monitoring and surveillance, high-precision image-guided automated assembly, and collision avoidance robotics require high bandwidth and extremely high throughput [1]. However, until recently, industrial communication mainly relied on wired Industrial Ethernet, which has a high installation cost and eliminates the option of flexible manufacturing. Moreover, the traditional existing sub-6 GHz wireless solutions like WiFi and 4G are unable to meet latency and throughput requirements [5]. Therefore, industrial embrace of millimeter-wave (mmWave) wireless communication is a game-changer towards extremely low latency and seamless connectivity [2]. With huge available bandwidth and low interference of mmWave bands, industries can capture near-real-time automation and other sophisticated applications [6]. The mmWave industrial communication can pave the way for new industrial automation capabilities alongwith huge room for high performance antenna design research.

Amongst the mmWave spectrum, worldwide unlicensed Industrial, Scientific and Medical (ISM) band around 60 GHz (57-66 GHz) has gained a lot of attention due to the demand for high data rate short-range indoor industrial wireless communication [7]. The development of IEEE 802.11ad and IEEE 802.11ay wireless standards has led to achieve multi-gigabit-per-second (mGbps) level communication at 60 GHz spectrum in the industrial environment [8], [9]. The complete 60 GHz band spans up to 71 GHz, and is divided into various channels, each with a minimum bandwidth of 2.16 GHz as shown in Fig. 1. However, in most geographical parts of the world, 57-66 GHz is utilized [1].

At 60 GHz mmWave ISM band, an efficient antenna design is of paramount importance because of a range of critical factors such as high path loss, compact size, and integration with frontend transceivers. Hence, antenna design must be low-cost, high-performance, compact, and easily integrateable for industrial and other commercial applications [10], [11]. Various types of antenna designs have been reported at 60 GHz band, such as on-chip antennas (AoC) and antennas-in-package (AiP) [12], LTCC-based antennas [13] and Printed Circuit Board (PCB)-based antennas [14]–[22], to list but a few. On-chip antennas suffer from high radiation losses and low gain due to low resistivity and high permittivity of silicon substrate [12]. LTCC-based antennas are complex to fabricate, expensive, and usually generate high surface waves because of high permittivity of LTTC materials due to which the radiation pattern of antenna is degraded and cross-coupling is increased. PCB-based antennas are low cost, less complex and provide easy integration with radio transceivers.

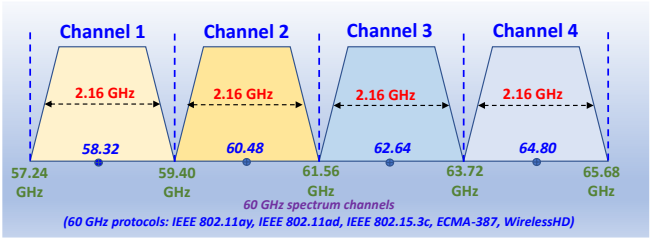

Fig. 1. A conceptual depiction of 60 GHz ISM band channel division from 57-66 GHz. Each channel occupies a bandwidth of 2.16 GHz.

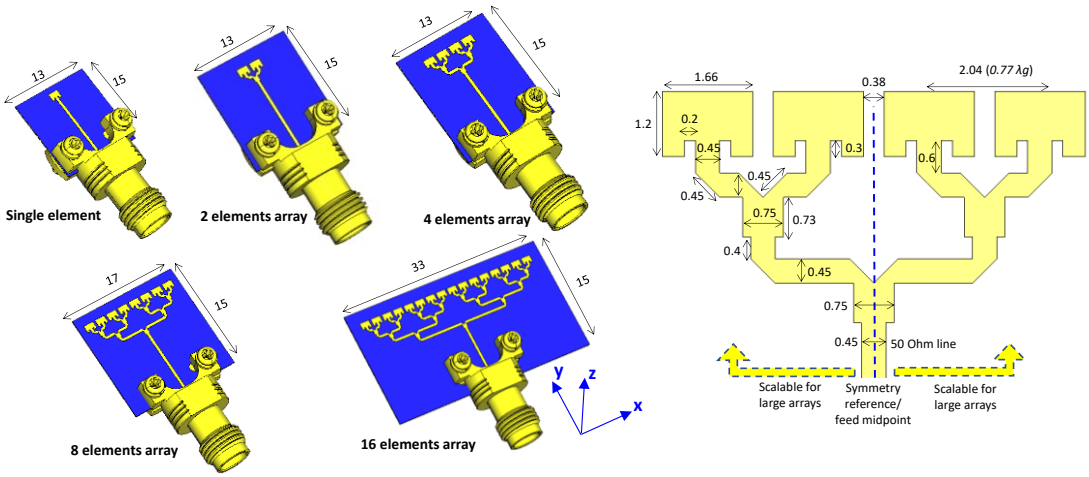

Fig. 2. Geometry of proposed array antennas with realistic connector model. Optimized dimensions of proposed feed network in millimeter. Following same dimensions, 2, 4, 8, and 16-element arrays are designed

In PCB-based mmWave antennas, the design of an efficient and wideband power divider (feed network) is always challenging. Even a minute change in the length of a feed junctions can affect array bandwidth and performance, because the wavelength is comparable with the dimensions of transmission lines. At mmWave bands, a beamforming antenna array with high gain is crucial to mitigate path loss. For instance, at 60 GHz, the free space path loss according to Friis transmission equation is 68 dB [10].

To address these challenges, we thoroughly analyze and elucidate the design of an improved 60 GHz beamforming array with high gain, wide bandwidth and stable radiation patterns. 2, 4, 8 and 16-element array configurations are designed and analyzed. High realized array gain of 16.5 dBi with a narrow beamwidth of 7° is achieved with 16-element array. The corporate feed network is designed and optimized to enhance array performance. Moreover, as the connector at mmWave practically affects the antenna radiation performance and cannot be neglected, therefore, a comprehensive analysis of the effect of the connector is also presented through co-simulations. Measurement results verify the simulated design.

II. Antenna Array Design And Analysis

The proposed antenna is designed on a low loss and high-performance Rogers 4003C substrate with dielectric constant of 3.55, thickness of 0.2 mm, dissipation factor of 0.0027, and copper thickness of 0.035 mm. A conventional rectangular microstrip patch antenna is employed as a basic radiator because of its low profile and planar geometry. The bottom side of the antenna has full copper layer acting as a ground plane, because of broadside beamforming intention. For impedance matching, inset cuts with optimized dimensions were introduced in the patch. The entire antenna array and feed network is designed and optimized to match

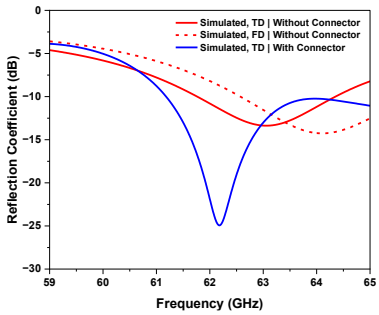

Fig. 3. Simulated reflection coefficient of single element antenna.

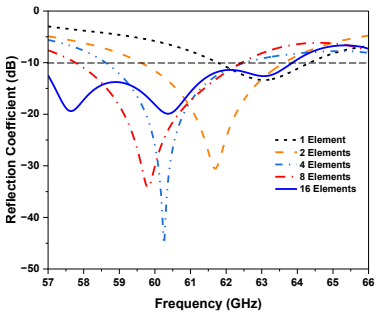

Fig. 4. Simulated reflection coefficient of array designs.

50 Ω impedance. After extensive parametric optimization, the finalized dimensions of the antenna prototype are presented in Fig. 2.

First, for the single element antenna design, time domain (TD) as well as frequency domain (FD) simulations were performed using full wave electromagnetic CST solver without connector. The simulated reflection coefficient of single element (TD) provides bandwidth of more than 2.16 GHz (61.77 – 64.4 GHz) as shown in Fig. 3. As expected, TD and FD reflection coefficients show shifted resonances. After that, the realistic connector model was co-simulated with the patch antenna as shown in Fig. 2. The antenna is fed through an edge launched 1.85 mm standard SMA

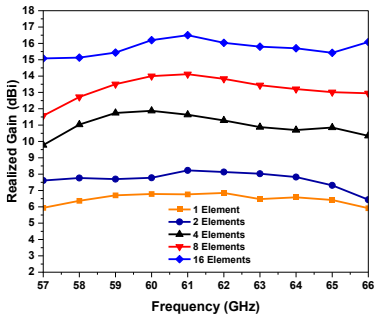

Fig. 5. Simulated realized gain of the proposed array antennas

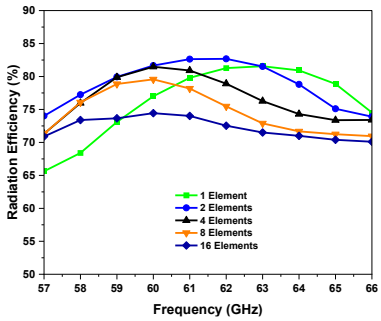

Fig. 6. Simulated radiation efficiency of the proposed array antennas.

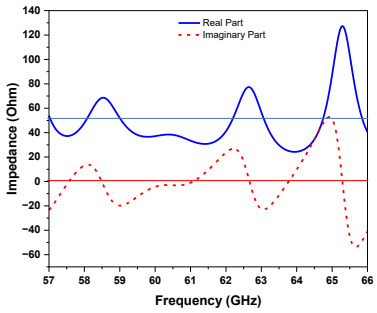

Fig. 7. Input impedance of the proposed 16-element array.

connector. The reflection coefficient with the inclusion of connector shows a redshift and a resonance occurs at 62.18 GHz, with -10 dB impedance bandwidth of 3 GHz (61.18 GHz to 64.2 GHz). The maximum realized gain of single element is 6.85 dBi at 62 GHz. The radiation pattern is towards broadside with very low cross polarization components in E and H-planes.

For the array design, the gap between consecutive antenna elements was optimized to be 2.04 mm (0.77 λ_g, where λ_g is the guided wavelength at 60 GHz). Quarter wave transmission line sections were used with optimized junction length of 0.73 mm to match the impedance of 50 Ω lines (0.45 mm). Since at the junction (where the array splits into two), 50 Ω line produces a parallel impedance effect and results in a virtual 25 Ω impedance point ($50 \times 50/(50 + 50)$). Then, quarter wave transmission line segments with an optimized width of 0.75 mm were used to match 25 Ω with 50 Ω. The sharp corners as well as junction points of the feed network were chamfered with the chamfering dimension of 0.45 mm. The chamfered transitions helped in smooth flow of the current and reduced spurious radiations from the feed network. The array is symmetrical around y-axis. The final optimized dimensions to construct high performance array topology are shown in Fig. 2. Starting from optimized 2-element array design, same scalability was used to construct higher array configurations. The minimum width of antennas (for 1, 2 and 4 elements array) is set as 13 mm to accommodate the connector, as the connector width is 12.2 mm. However, the length of all array topologies is set as 15 mm because of linear array configuration. Such configuration helped in compact array size in y-direction.

The simulated reflection coefficients of array antennas are shown in Fig. 4. The -10 dB impedance bandwidth for 2, 4, 8 and 16-element array is from 59.61-63.62 GHz, 58.62-62.53 GHz, 57.77-62.43, and 57-64 GHz respectively. The 16-element array provides the wide impedance bandwidth of 7 GHz. It can be noted from Fig. 4 that two resonances occur at 57.4 and 60.48 GHz for 16-element array, due to which wideband response is achieved. Remember that 60.48 GHz is the center frequency of Channel 2 (Fig. 1).

The simulated peak realized gains for 2, 4, 8 and 16-element arrays are 8.23, 11.63, 14.11 and 16.5 dBi

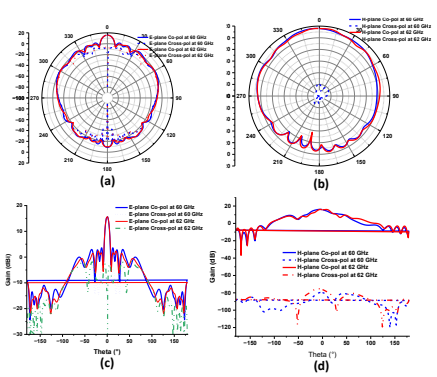

Fig. 8. (a) (polar) E-plane co and cross-pol components at 60 and 62 GHz. (b) (polar) H-plane co and cross-pol components at 60 and 62 GHz. (c) (cartesian) E-plane co and cross-pol components at 60 and 62 GHz. (d) (cartesian) H-plane co and cross-pol components at 60 and 62 GHz.

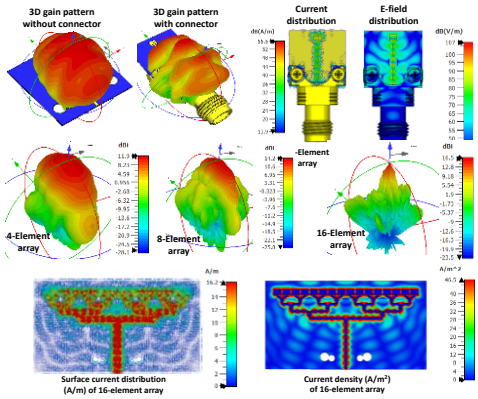

Fig. 9. (top) 3-D gain patterns and curent distribution of single elment with and without connector at 61 GHz. (mid) 3-D gain patterns of array geometries at 61 GHz. (bottom) surface current distribution and current density of 16-element array at 61 GHz show confined current energy and less spurious radiations from feed network.

respectively at 61 GHz. The realized gain for 16-element array is greater than 15 dBi in the whole covered band. A fair comparison of realized gain for different array configurations is depicted in Fig. 5. The radiation efficiency for all array antennas is above 70% in the covered bandwidth as shown in Fig. 6. As depicted in Fig. 7, the input impedance of 16-element array shows multiple resonances with its real part averaged at 50 Ω, and imaginary part around zero (analogous to sinusoidal signal resonance between a maximum and minimum value, with an average value of zero over a cycle). This confirms the well-matched response of the proposed array over a wide bandwidth.

The half-power beamwidth (HPBW) in x-z plane (phi 0°) for 1, 2, 4, 8 and 16-element arrays is 78.5°, 57.3°, 31.4°, 15.7° and 7.7° respectively at 61 GHz. The main lobes are directed towards the broadside and the side-lobe levels (SLL) are well below -10 dB for all array geometries. The HPBWs are relatively higher in y-z plane (phi 90°) for the obvious reason of linear array configuration. 2-D polar and cartesian gain patterns of the proposed 16-element array at 60 and 62 GHz, are shown in Fig. 8. The cross-polarization level is quite low around the broadside for E-plane, and throughout low for H-plane due to carefully designed symmetrical nature of the proposed geometry. The radiation patterns are quite stable in the whole band for all array topologies. 3-D gain patterns at 61 GHz for different array topologies are shown in Fig. 9 (mid). High broadside beamforming gain for the 16-element array is witnessed.

The effect of connector is demonstrated in Fig. 9 (top), which reveals that the presence of connector distorts the radiation pattern due to additionally generated surface waves. In order to mitigate this effect, a longer feed line (while taking care of impedance matching) may be used to create a sufficient distance between the connector and the radiating elements. The surface current distribution of the 16-element array at 61 GHz is shown in Fig. 9 (bottom), from which it can be noticed that maximum current density is confined within the feed network and spurious radiations from the feed network are the least. This results in high radiation efficiency and high array gain.

III. Measurement Results

The measured reflection coefficients for single element and 16-element array are shown in Fig. 10, and show quite good agreement with the simulation results. The fabricated prototypes are shown in Fig. 11. The measured -10 dB impedance bandwidth for single element and 16-element array is from 59.89-64.59 GHz and 56.88-64.4 GHz respectively. As revealed, the measurement results majorly match with the simulations results with included connector. Some deviations in the measured results are due to surface roughness and fabrication tolerance as shown by Fig. 11.

TABLE I. PERFORMANCE COMPARISON OF THE PROPOSED ARRAY WITH OTHER RELATED WORKS.

Ref.	-10 dB impedance BW (GHz)	Peak gain (dBi)	Array topology	Efficiency (%)	Size array (mm × mm)
[14]	59.3-61.8	22	Complex 12-way SIW array	68	Not reported
[15]	54.6-71.2	16	4 × 4	NA	14 × 16
[16]	55-68	15.6	4 × 4	67	20 × 20
[17]	59.2-60.4	20.6	32 (4 × 8)	78	17 × 22.5
[18]	57-62.8	11.6	1 × 2	85	20.64 × 20
[19]	57.5-60.7	18	4 × 4	NA	18.5 × 30
[20]	58-61.3	13	2 × 2	NA	10.5 × 10.5
This Work	**55-64**	**16.5**	**1 × 16**	**>75**	**15×33**

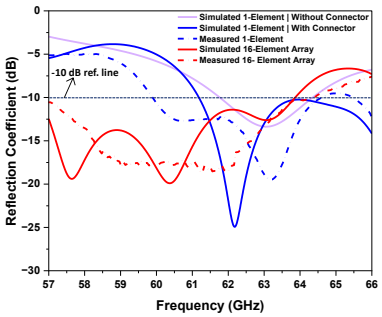

Fig. 10. Measured and simulated reflection coefficients of proposed single element and 16-element array.

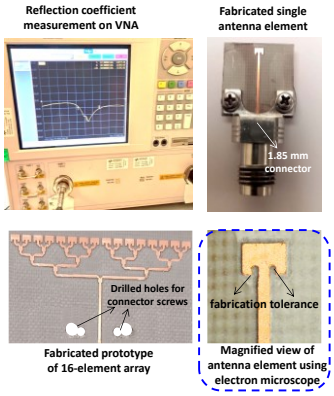

Fig. 11. Measurement setup alongwith fabricated prototypes. The magnified image was captured using an electron microscope which reveals surface roughness and fabrication tolerance.

The antenna prototypes were fabricated in LPKF ProtoMat S103® milling machine. A magnified image of the patch antenna was captured using an electron microscope and shown in Fig. 11. Instead of right-angled sharp inset cuts (as designed in simulations), rounded inset cuts are noted in the fabricated prototype due to limitations of milling bits. The deviations in the measurement results as compared to those of simulations are mainly due to this effect.

The radiation pattern, gain and SLL measurements are not included in this work due to brevity and will be the part of the future extension of this work. A performance

comparison of the proposed array antenna design is presented in Table I.

IV. Conclusion

In this paper, the design of a compact and high-performance planar beamforming array is presented. A thorough analysis of the array antenna performance is presented using full-wave realistic simulations. A high beamformed realized gain of 16.5 dBi at 61 GHz, with peak radiation efficiency of 75%, and wide impedance bandwidth from 55-64 GHz is achieved for 16-element array. The cross polarized levels and SLLs are quite low. Moreover, the realistic connector model is co-simulated with antenna and its effect on the radiation pattern and bandwidth is analyzed. The measured reflection coefficient of proposed antenna matches quite well with that of simulations. The proposed antenna array is a suitable candidate for multi-gigabit-per-second industrial applications such as intelligent logistics, intelligent manufacturing, remote visual monitoring and surveillance, high-precision image-guided automated assembly, and collision avoidance robotics in smart industries. The thorough analysis of the proposed antenna array serves as a catalyst for improved antenna array designs at mmWave bands.

Acknowledgment

This work was supported by Innovative and Collaborative Research Grant under Pakistan UK Education Gateway (ICRG-2020) Project No. 310366 - Deforestation in Pakistan: Combating through Wireless Sensor Networks (DePWiSeN).

References

[1] M. Cheffena, "Industrial wireless communications over the millimeter wave spectrum: opportunities and challenges," *IEEE Commun. Mag.*, vol. 54, no. 9, pp. 66–72, 2016.

[2] S. Saponara, F. Giannetti, B. Neri, and G. Anastasi, "Exploiting mm-wave communications to boost the performance of industrial wireless networks," *IEEE Trans. Ind. Informatics*, vol. 13, no. 3, pp. 1460–1470, 2017.

[3] X. Wang *et al.*, "Millimeter wave communication: A comprehensive survey," *IEEE Commun. Surv. Tutorials*, vol. 20, no. 3, pp. 1616–1653, 2018, doi: 10.1109/COMST.2018.2844322.

[4] A. Jabbar *et al.*, "Millimeter-Wave Smart Antenna Solutions for URLLC in Industry 4.0 and Beyond," *Sensors*, vol. 22, no. 7, p. 2688, 2022.

[5] Q. Wang and J. Jiang, "Comparative examination on architecture and protocol of industrial wireless sensor network standards," *IEEE Commun. Surv. \& Tutorials*, vol. 18, no. 3, pp. 2197–2219, 2016.

[6] A. Hottinen, M. Kuusela, K. Hugl, J. Zhang, and B. Raghothaman, "Industrial embrace of smart antennas and MIMO," *IEEE Wirel. Commun.*, vol. 13, no. 4, pp. 8–16, 2006.

[7] C. Pielli, T. Ropitault, and M. Zorzi, "The potential of mmwaves in smart industry: Manufacturing at 60 ghz," in *International Conference on Ad-Hoc Networks and Wireless*, 2018, pp. 64–76.

[8] P. Zhou *et al.*, "IEEE 802.11 ay-based mmWave WLANs: Design challenges and solutions," *IEEE Commun. Surv. \& Tutorials*, vol. 20, no. 3, pp. 1654–1681, 2018.

[9] Y. Ghasempour, C. R. C. M. Da Silva, C. Cordeiro, and E. W. Knightly, "IEEE 802.11ay: Next-Generation 60 GHz Communication for 100 Gb/s Wi-Fi," *IEEE Commun. Mag.*, vol. 55, no. 12, pp. 186–192, 2017, doi: 10.1109/MCOM.2017.1700393.

[10] T. S. Rappaport, J. N. Murdock, and F. Gutierrez, "State of the art in 60-GHz integrated circuits and systems for wireless communications," *Proc. IEEE*, vol. 99, no. 8, pp. 1390–1436, 2011, doi: 10.1109/JPROC.2011.2143650.

[11] R. C. Daniels, J. N. Murdock, T. S. Rappaport, and R. W. Heath, "60 GHz wireless: Up close and personal," *IEEE Microw. Mag.*, vol. 11, no. 7, pp. 44–50, 2010.

[12] H. M. Cheema and A. Shamim, "The last barrier: on-chip antennas," *IEEE Microw. Mag.*, vol. 14, no. 1, pp. 79–91, 2013.

[13] U. Ullah, N. Mahyuddin, Z. Arifin, M. Z. Abdullah, and A. Marzuki, "Antenna in LTCC technologies: a review and the current state of the art," *IEEE Antennas Propag. Mag.*, vol. 57, no. 2, pp. 241–260, 2015.

[14] X.-P. Chen, K. Wu, L. Han, and F. He, "Low-cost high gain planar antenna array for 60-GHz band applications," *IEEE Trans. Antennas Propag.*, vol. 58, no. 6, pp. 2126–2129, 2010.

[15] H. Sun, Y.-X. Guo, and Z. Wang, "60-GHz circularly polarized U-slot patch antenna array on LTCC," *IEEE Trans. Antennas Propag.*, vol. 61, no. 1, pp. 430–435, 2012.

[16] W. Yang, K. Ma, K. S. Yeo, and W. M. Lim, "A compact high-performance patch antenna array for 60-GHz applications," *IEEE Antennas Wirel. Propag. Lett.*, vol. 15, pp. 313–316, 2015.

[17] H. Chu, J.-X. Chen, and Y.-X. Guo, "An efficient gain enhancement approach for 60-GHz antenna using fully integrated vertical metallic walls in LTCC," *IEEE Trans. Antennas Propag.*, vol. 64, no. 10, pp. 4513–4518, 2016.

[18] T. S. Mneesy, R. K. Hamad, A. I. Zaki, and W. A. E. Ali, "A novel high gain monopole antenna array for 60 GHz millimeter-wave communications," *Appl. Sci.*, vol. 10, no. 13, p. 4546, 2020.

[19] Y. Al-Alem and A. A. Kishk, "Low-profile low-cost high gain 60 GHz antenna," *IEEE Access*, vol. 6, pp. 13376–13384, 2018.

[20] B. Biglarbegian, M. Fakharzadeh, D. Busuioc, M.-R. Nezhad-Ahmadi, and S. Safavi-Naeini, "Optimized microstrip antenna arrays for emerging millimeter-wave wireless applications," *IEEE Trans. Antennas Propag.*, vol. 59, no. 5, pp. 1742–1747, 2011.

[21] Y. Al-Alem and A. A. Kishk, "Efficient millimeter-wave antenna based on the exploitation of microstrip line discontinuity radiation," *IEEE Trans. Antennas Propag.*, vol. 66, no. 6, pp. 2844–2852, 2018.

[22] A. Jabbar, Q. H. Abbasi, M. Ali Imran, and M. U. Rehman, "Design of a 60 GHz Antenna for Multi-Gigabit WiGig Communication in Industry 4.0," in *2022 IEEE AP-S/URSI*, 2022, pp. 325–326, doi: 10.1109/AP-S/USNC-URSI47032.2022.9886405.